

# Control System Analysis of the *Triangle*

dc&e

May 1, 2025\*

## Contents

<b>1</b>	<b>Introduction</b>	<b>3</b>
<b>2</b>	<b>Differential equations the <i>Triangle</i></b>	<b>3</b>
2.1	Construction of the Lagrangian . . . . .	3
2.2	Equations of motion . . . . .	4
2.3	First order form . . . . .	6
<b>3</b>	<b>Stability analysis and controller design</b>	<b>6</b>
3.1	A global asymptotic controller . . . . .	6
3.2	Passivity Property of the System . . . . .	7
3.3	Energy Based Swing-Up Controller . . . . .	8
3.4	Another Swing-up controller . . . . .	10
3.4.1	Determination of the wheel's speed for swing-up . . . . .	11
3.4.2	Determination of switching thresholds . . . . .	12
<b>4</b>	<b>Learning Based Control (Experiments)</b>	<b>13</b>
4.1	Data Generation from NMPC . . . . .	13
4.2	Imitation Learning Approaches . . . . .	15

## Preface

This work was carried out by **dc&e**, with contributions from:

1. Himanshu Paudel

# 1 Introduction

We present the mathematical modeling, control system design, and theoretical analysis of the *Triangle* balance robot.

## 2 Differential equations the *Triangle*

In this section, we develop the mathematical model of the *Triangle*, i.e., derive its differential equations. These equations form the basis for stability analysis, control design, and simulation of the control system.

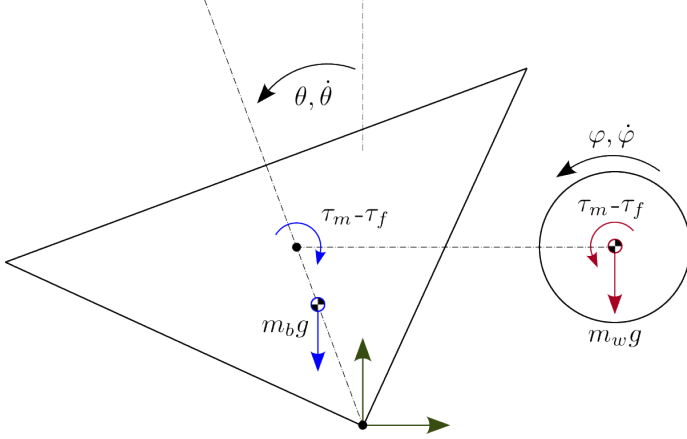


Figure 1: Forces and torques acting on the *Triangle* Balance. Figure inspired from [1]

Fig.(1) shows the free-body diagram of the *Triangle* where the parameters are defined as following:

$$\begin{aligned}
 \theta &= \text{Pendulum angle} \\
 \varphi &= \text{Wheel angle relative to pendulum} \\
 m_b, I_b, l_b &= \text{Mass, inertia, and center of mass height of pendulum body} \\
 m_w, I_w, l_w &= \text{Mass, inertia, and center of mass height of wheel} \\
 \tau_m &= \text{Motor torque} \\
 \tau_f &= \text{Friction torque} \\
 M &= m_b l_b + m_w l_w \\
 I &= I_b + m_b l_b^2 + m_w l_w^2
 \end{aligned}$$

### 2.1 Construction of the Lagrangian

Euler-Lagrange equation is used to derive the differential equation, therefore, we start by expressing the Kinetic energy  $T$  and potential energy  $V$  of the *Triangle* to compute the Lagrangian as

$$L = T - V \quad (1)$$

The kinetic energy of the *Triangle* is the sum of kinetic energy of the body  $T_b$ , and that of the wheel  $T_w$ . The term  $T_b$  can be expressed as the sum of the kinetic energy due to the angular motion and the translational motion of the body's center of mass i.e.

$$T_b = \frac{1}{2} (I_b + m_b l_b^2) \dot{\theta}^2 \quad (2)$$

where,  $l_b\dot{\theta}$  is the linear velocity of the center of mass.<sup>1</sup>

The reaction wheel, on the other hand, has three sources of its kinetic energy: (1) rotation about its own axis, (2) rotation of the body about its axis, and (3) translational motion in the inertial frame, resulting from the body's rotation. Therefore, the kinetic energy of the wheel is the sum of its rotational and the translational kinetic energies i.e.

$$T_w = \frac{1}{2} \left( I_w(\dot{\theta} + \dot{\varphi})^2 + m_w l_w^2 \dot{\theta}^2 \right). \quad (3)$$

The total kinetic energy of the *Triangle* can be expressed as

$$\begin{aligned} T &= T_b + T_w \\ &= \frac{1}{2} (I_b + m_b l_b^2) \dot{\theta}^2 + \frac{1}{2} (I_w(\dot{\theta} + \dot{\varphi})^2 + m_w l_w^2 \dot{\theta}^2) \\ &= \frac{1}{2} ((I_b + m_b l_b^2 + I_w + m_w l_w^2) \dot{\theta}^2 + 2I_w \dot{\theta} \dot{\varphi} + I_w \dot{\varphi}^2) \\ &= \frac{1}{2} (I \dot{\theta}^2 + I_w \dot{\theta}^2 + 2I_w \dot{\theta} \dot{\varphi} + I_w \dot{\varphi}^2) \\ &= \frac{1}{2} (I \dot{\theta}^2 + I_w(\dot{\theta} + \dot{\varphi})^2) \end{aligned} \quad (4)$$

where,  $I = I_b + m_b l_b^2 + m_w l_w^2$ .

We know that a mass' potential energy depends on its vertical position (the good old  $-mgh$ ). Both the body and the wheel rotates with the same angle  $\theta$  with respect to the vertical. Therefore, as the body rotates, both center of mass move in a circular arc of radius  $l_b$  and  $l_w$  respectively. The vertical height of each center of mass relative to the pivot is:

$$\begin{aligned} h_b &= -l_b \cos \theta \\ h_w &= -l_w \cos \theta \end{aligned}$$

where the terms are negative because  $\theta = 0$ . The total potential energy of the *Triangle* is the sum of potential energies of the body and the wheel, i.e.

$$\begin{aligned} V &= -m_b g h_b - m_w g h_w \\ &= -(m_b g l_b + m_w g l_w) \cos \theta \\ &= -M g \cos \theta \end{aligned} \quad (5)$$

where,  $M = m_b l_b + m_w l_w$ .

We can now use Eqn.(1) to compute the Lagrangian.

$$L = T - V = \frac{1}{2} I \dot{\theta}^2 + \frac{1}{2} I_w(\dot{\theta} + \dot{\varphi})^2 + M g \cos \theta \quad (6)$$

## 2.2 Equations of motion

### Equation of motion of the body

The Euler-Lagrange equation for the body is expressed as

$$\frac{d}{dt} \left( \frac{\partial L}{\partial \dot{\theta}} \right) - \frac{\partial L}{\partial \theta} = \tau_f - \tau_m. \quad (7)$$

---

<sup>1</sup>If a rigid body rotates around a fixed point with angular velocity  $\dot{\theta}$ , any point on the body located at a distance  $r$  from the pivot traces a circular path. The linear velocity  $v$  of that point is related to the angular velocity as  $v = r\dot{\theta}$ .

Computing the terms involved.

$$\begin{aligned}\frac{\partial L}{\partial \dot{\theta}} &= I\dot{\theta} + I_w(\dot{\theta} + \dot{\varphi}) \implies \frac{d}{dt} \left( \frac{\partial L}{\partial \dot{\theta}} \right) = (I + I_w)\ddot{\theta} + I_w\ddot{\varphi} \\ \frac{\partial L}{\partial \theta} &= -Mg \sin \theta\end{aligned}\tag{8}$$

Plugging in the terms to Eqn.(7), we get the equation of motion of the body.

$$(I + I_w)\ddot{\theta} + I_w\ddot{\varphi} - Mg \sin \theta = 0\tag{9}$$

### Equation of motion of the wheel

The Euler-Lagrange equation for the wheel is expressed as

$$\frac{d}{dt} \left( \frac{\partial L}{\partial \dot{\varphi}} \right) - \frac{\partial L}{\partial \varphi} = \tau_f - \tau_m.\tag{10}$$

Similar to what we did for the body, computing the terms involved,

$$\begin{aligned}\frac{\partial L}{\partial \dot{\varphi}} &= I_w(\dot{\theta} + \dot{\varphi}) \implies \frac{d}{dt} \left( \frac{\partial L}{\partial \dot{\varphi}} \right) = I_w(\ddot{\theta} + \ddot{\varphi}) \\ \frac{\partial L}{\partial \varphi} &= 0\end{aligned}\tag{11}$$

Plugging the expression into the Eqn.(10), we get

$$\begin{aligned}I_w(\ddot{\theta} + \ddot{\varphi}) &= \tau_m - \tau_f \\ \implies \ddot{\varphi} &= \frac{\tau_m - \tau_f}{I_w} - \ddot{\theta}\end{aligned}\tag{12}$$

### Equations of motion of the system

We can observe that equation of motion of both body and the wheel are coupled with double derivatives as both Eqn.(9) and Eqn.(12) contains both terms  $\ddot{\theta}$  and  $\ddot{\varphi}$ . Now we will derive separate equation of motion for each of them by decoupling the double derivative terms.

We begin by plugging Eqn.(12) into Eqn.(9).

$$\begin{aligned}(I + I_w)\ddot{\theta} + I_w \left( \frac{\tau_m - \tau_f}{I_w} - \ddot{\theta} \right) + Mg \sin \theta &= \tau_f - \tau_m \\ I\ddot{\theta} &= Mg \sin \theta - \tau_m + \tau_f \\ \implies \ddot{\theta} &= \frac{Mg \sin \theta - \tau_m + \tau_f}{I}\end{aligned}\tag{13}$$

Plugging the expression in Eqn.(12) gives us

$$\ddot{\varphi} = \frac{(I + I_w)(\tau_m - \tau_f)}{II_w} - \frac{Mg \sin \theta}{I}\tag{14}$$

Eqn.(13) and Eqn.(14) are the equations of motion of the *Triangle*.

## 2.3 First order form

$$\frac{d}{dt} \begin{bmatrix} \theta \\ \dot{\theta} \\ \phi \\ \dot{\phi} \end{bmatrix} = \begin{bmatrix} \dot{\theta} \\ \frac{-\tau_m + \tau_f}{I} + \frac{Mg \sin \theta}{I} \\ \dot{\phi} \\ \frac{(\tau_m - \tau_f)(I + I_w)}{IIw} - \frac{Mg \sin \theta}{I} \end{bmatrix}$$

## 3 Stability analysis and controller design

The goal of this section is to design control law for the *Triangle* by using the mathematical tools of the control theory by trying our best to prove our assumptions so that we are comfortable with what we believe.

The goal of the controller is to regulate  $\theta$ ,  $\dot{\theta}$ , and  $\dot{\varphi}$  to zero. We're not concerned with  $\varphi$  at the moment—that's something for a future project. We will begin by performing mathematical analysis proving why we cannot have smooth single control law which can swing up and balance the *Triangle*. That being done, we are naturally lead to implementing two controllers, one for the swing-up and the next for stabilization. Each of them are discussed in detail. Finally, the question of when to switch from swing-up to stabilization is addressed.

### 3.1 A global asymptotic controller

Brockett's Law provides the necessary condition for the existence of a continuously differentiable control law for nonlinear systems. In this case, however, we attempt to disprove Brockett's condition to show that a single continuously differentiable time invariant control law does not exist. This leads to the popular conclusion that two controllers are needed—one for swing-up and the other for stabilization. It should be noted that a single continuous controller cannot accomplish both tasks, but if the controller is a discontinuous function, it might. Therefore, our approach is more like: "We are acquainted with continuous control design techniques. First, we will check if this can be done. If not, we will settle for two different controllers, one for swing-up and the other for stabilization."

**Brockett's conditions** Let  $\dot{x} = f(x, u)$  be given, with  $f(x_0, 0) = 0$ , and  $f(\cdot, \cdot)$  continuously differentiable in a neighborhood of  $(x_0, 0)$ . A necessary condition for the existence of a continuously differentiable control law which makes  $(x_0, 0)$  asymptotically stable is that:

1. The linearized system should have no uncontrollable modes associated with eigenvalues whose real part is positive.
2. There exists a neighborhood  $\mathcal{N}$  of  $(x_0, 0)$  such that for each  $\zeta \in \mathcal{N}$ , there exists a control  $u_\zeta(\cdot)$  defined on  $[0, \infty)$  such that this control steers the solution of  $\dot{x} = f(x, u_\zeta)$  from  $x = \zeta$  at  $t = 0$  to  $x = x_0$  at  $t \rightarrow \infty$ .
3. The mapping  $\gamma : A \times \mathbb{R}^m \rightarrow \mathbb{R}^n$ , defined by  $\gamma : (x, u) \rightarrow f(x, u)$ , should be onto an open set containing 0 .

Now, for the first condition , starting from the state space/first order form:

$$\frac{d}{dt} \begin{bmatrix} \theta \\ \dot{\theta} \\ \phi \\ \dot{\phi} \end{bmatrix} = \begin{bmatrix} \dot{\theta} \\ \frac{-\tau_m + \tau_f}{I} + \frac{Mg \sin \theta}{I} \\ \dot{\phi} \\ \frac{(\tau_m - \tau_f)(I + I_w)}{IIw} - \frac{Mg \sin \theta}{I} \end{bmatrix}$$

Linearizing this system, we get:

Now, the characteristic equation of this system is given by:

$$\det(\lambda I - A) = 0$$

Upon Solving this equation, we get four roots as:

$$\lambda = 0, 0, i\sqrt{\frac{Mg}{I}}, -i\sqrt{\frac{Mg}{I}}$$

For determining the uncontrollable nodes, we would need to check controllability and use the Kalman decomposition or compute the PBH (Popov–Belevitch–Hautus) test, but in this case since there is no eigenvalue with Real part ,the first condition of Brockett's condition is satisfied.

Moving on, for the third condition of Brockett's condition, we intend to show that the mapping from  $\gamma : (x, u) \rightarrow f(x, u)$  is not onto an open set containing 0.

$$\frac{d}{dt} \begin{bmatrix} \theta \\ \dot{\theta} \\ \phi \\ \dot{\phi} \end{bmatrix} = \begin{bmatrix} \dot{\theta} \\ \frac{-\tau_m + \tau_f}{I} + \frac{Mg \sin \theta}{I} \\ \dot{\phi} \\ \frac{(\tau_m - \tau_f)(I + I_w)}{IIw} - \frac{Mg \sin \theta}{I} \end{bmatrix} = \begin{bmatrix} f_1 \\ f_2 \\ f_3 \\ f_4 \end{bmatrix} \text{ (say)}$$

Now, taking the sum of the second and the third term:

$$f_2 + f_4 = -\frac{\tau_m + \tau_f}{I} + \frac{Mg \sin \theta}{I} + \frac{(\tau_m - \tau_f)(I + I_w)}{IIw} - \frac{Mg \sin \theta}{I}$$

Simplifying this equation, we get:

$$f_2 + f_4 = \frac{\tau_m - \tau_f}{I_w}$$

This shows that  $f_2$  and  $f_4$  can only appear in pair due to them having to satisfy the above sum condition. Hence, the co-domain of the function is not equal to the range and the function is not onto which is a clear case of violation of the Brockett's necessary condition and thus a single continuously differentiable control law cannot stabilize the system.

### 3.2 Passivity Property of the System

The total energy of the Triangle system, which consists of the pendulum body and the wheel, is the sum of its kinetic and potential energies:

$$E = T + V \quad (15)$$

where the kinetic energy is

$$T = \frac{1}{2}(I_b + m_b l_b^2 + I_w + m_w l_w^2)\dot{\theta}^2 + I_w \dot{\theta} \dot{\phi} + \frac{1}{2}I_w \dot{\phi}^2, \quad (16)$$

and the potential energy due to gravity is

$$V = -Mg \cos \theta, \quad M = m_b l_b + m_w l_w. \quad (17)$$

Thus, the total energy can be written explicitly as

$$E = \frac{1}{2}(I_b + m_b l_b^2 + I_w + m_w l_w^2) \dot{\theta}^2 + I_w \dot{\theta} \dot{\phi} + \frac{1}{2} I_w \dot{\phi}^2 - Mg \cos \theta. \quad (18)$$

Taking the time derivative of the total energy, we obtain

$$\dot{E} = (I_b + m_b l_b^2 + I_w + m_w l_w^2) \ddot{\theta} \dot{\theta} + I_w (\dot{\theta} \ddot{\phi} + \dot{\phi} \ddot{\theta}) + I_w \dot{\phi} \ddot{\phi} + Mg \sin \theta \dot{\theta}. \quad (19)$$

Substituting the Euler-Lagrange equations of motion for the system from Eqn.(13) and Eqn.(14).

$$\dot{E} = \dot{\phi} \tau_m. \quad (20)$$

We have also considered the absence of friction torque  $\tau_f$  and  $\tau$  is equal to  $\tau_m$  for the following sections. This expression shows that the rate of change of total energy is equal to the power supplied by the motor torque, and therefore the system satisfies the **passivity property**.

### 3.3 Energy Based Swing-Up Controller

#### Lyapunov function

The Lyapunov candidate function is defined as

$$V = \frac{1}{2} k_E E^2 + \frac{1}{2} k_v \dot{\phi}^2 + \frac{1}{2} k_p \phi^2 \quad (21)$$

Taking the time derivative of  $V$ ,

$$\dot{V} = k_E E \dot{E} + k_v \dot{\phi} \ddot{\phi} + k_p \phi \dot{\phi} \quad (22)$$

Using the relation from passivity property in eqn. (20) we obtain

$$\dot{V} = k_E E \tau \dot{\phi} + k_v \dot{\phi} \ddot{\phi} + k_p \phi \dot{\phi} \quad (23)$$

$$\dot{V} = \dot{\phi} (k_E E \tau + k_v \ddot{\phi} + k_p \phi) \quad (24)$$

Using the system dynamics given by Eqn.(13) and Eqn.(14), we get

$$\dot{V} = \dot{\phi} \left[ k_E E \tau + k_v \tau \left( \frac{I + I_w}{II_w} \right) - k_v \frac{mgl}{I} \sin \phi + k_p \phi \right] \quad (25)$$

Let,

$$k_1 = k_v \frac{I + I_w}{II_w}, \quad k_2 = k_v \frac{mgl}{I} \quad (26)$$

$$\dot{V} = \dot{\phi} [\tau(k_E E + k_1) - k_2 \sin \phi + k_p \phi] \quad (27)$$

## Control Design

Assume the control input satisfies

$$\tau(k_E E + k_1) - k_2 \sin \phi + k_p \phi = -k_d \dot{\phi} \quad (28)$$

Then the Lyapunov derivative becomes

$$\dot{V} = -k_d \dot{\phi}^2 \quad (29)$$

which is negative semi-definite.

Solving (28) for  $\tau$ , the control law is obtained as

$$\tau = \frac{-k_d \dot{\phi} - k_p \phi + k_2 \sin \phi}{k_E E + k_1} \quad (30)$$

For the case  $\dot{V} = 0$ , LaSalle's invariance principle is invoked to analyze the asymptotic behavior of the system.

## LaSalle's Invariance Principle Analysis

The Lyapunov derivative satisfies

$$\dot{V} = -k_d \dot{\phi}^2 \leq 0. \quad (31)$$

Hence,  $V(t)$  is non-increasing and all closed-loop trajectories are bounded.

Define a compact, positively invariant set  $\Omega$  such that all trajectories evolve in  $\Omega$ . Let

$$\mathcal{I} = \{x \in \Omega \mid \dot{V}(x) = 0\}. \quad (32)$$

From  $\dot{V} = -k_d \dot{\phi}^2$ , it follows that

$$\mathcal{I} = \{x \in \Omega \mid \dot{\phi} = 0\}.$$

Let  $\mathcal{M}$  denote the largest invariant set contained in  $\mathcal{I}$ . By LaSalle's invariance principle, every closed-loop trajectory starting in  $\Omega$  approaches  $\mathcal{M}$  as  $t \rightarrow \infty$ .

In the set  $\mathcal{I}$ ,  $\dot{\phi} = 0$  and therefore  $\phi$  is constant. Since

$$\dot{E} = \tau \dot{\phi},$$

the energy  $E$  is also constant on  $\mathcal{I}$ .

Consequently, all system trajectories converge to the largest invariant set  $\mathcal{M} \subseteq \{\dot{\phi} = 0\}$ .

## The stabilizer control law

For our stabilizer control law, first term compensates gravity, second damps the robot velocity, third compensates friction, and the last damps the wheel velocity. If we are near the equilibrium angle, then gravity compensation can be considered linear with the approximation  $\sin \theta \approx \theta$  which linearizes the control law to be

$$\tau_m = k_p \theta + k_d \dot{\theta} + k_w \dot{\varphi} - \tau_f. \quad (33)$$

This requires us to determine the friction of the motor. However, the classic action of neglecting friction leads to simpler linear control law

$$\tau_m = k_p \theta + k_d \dot{\theta} + k_w \dot{\varphi} \quad (34)$$

### 3.4 Another Swing-up controller

The goal of the swing-up controller is to “wake up” the *Triangle* from its stable equilibrium and bring it closer to the upright position, enabling the stabilizer to take over and perform the actual balancing. In this section, we discuss and design the swing-up controller, beginning with physical intuition and mathematical analysis to identify key parameters.

Our study of swing-up controllers naturally began with studying the swing-up of the classic inverted pendulum or the Furuta pendulum. Therefore, we will start our analysis with the swing-up for those pendulums and make some inferences about what the swing-up for the *Triangle* looks like—or rather, does not look like.

#### Swing-up for inverted pendulum and Furuta pendulum

Figs. 2A and B show schematic diagrams of the Furuta pendulum and the cart-pole inverted pendulum system. The Furuta pendulum consists of a motorized rotating base to which a passive pendulum is attached via a bearing. The pendulum is unactuated and responds to the angular motion of the base. Swing-up is achieved by oscillating the base back and forth, thereby injecting energy into the pendulum until it enters the vicinity of the upright position, where a stabilizing controller can take over.

Similarly, Figs. 2C and D depict the cart-pole system, where linear translation of a cart on a belt emulates base rotation. As with the Furuta pendulum, the swing-up phase consists of back-and-forth motion of the cart to accumulate energy in the pendulum.

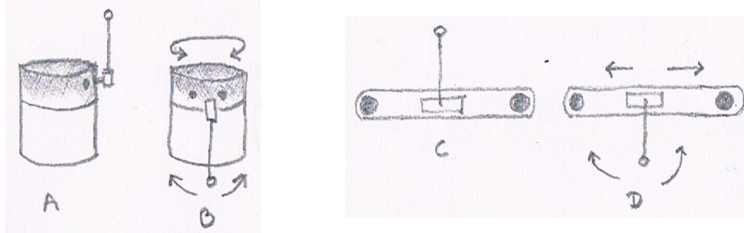


Figure 2: A: Balanced Furuta pendulum. B: Swing-up of Furuta pendulum.  
C: Balanced inverted pendulum. D: Swing-up of inverted pendulum.

In both classical cases, two crucial properties enable successful swing-up:

1. The pendulum’s motion is directly influenced by external torques applied to the base. The energy required for swing-up is externally supplied.
2. The pendulum is free to swing around the stable equilibrium (hanging down), allowing multiple passes through the bottom position to gradually increase its energy.

In contrast, the *Triangle* is based on a fundamentally different actuation and configuration setup:

- **Momentum-based actuation:** It relies on internal actuation via a reaction wheel. This means that the pendulum’s motion results from internal momentum exchange, not direct torque on a pivoted base.
- **Restricted motion domain:** Due to the geometry of the triangle-shaped body, the system cannot rotate freely around the stable equilibrium point. The body rests flat on the ground and cannot swing through the downward position repeatedly. As a result, traditional energy-pumping swing-up strategies—which rely on oscillating the pendulum around its lowest point—are not applicable.
- **No natural oscillating cycle:** Once the *Triangle* body falls to the ground, there is no passive return to a previous state without deliberate re-actuation. This lack of reversible dynamics further invalidates classical swing-up methods.

## Swing-up for the *Triangle*

Based on the intuition developed above, it is clear that a fundamentally different approach is required for swing-up control in the *Triangle*. Unlike conventional systems that exploit natural dynamics and repeated oscillations, the controller must instead perform a deliberate, one-shot energy transfer from the reaction wheel to the body. One possible method is to plan a trajectory from the resting position to the upright configuration and follow it using a precomputed, learned, or real-time trajectory optimization. While this approach can yield smooth motion, it is highly sensitive to model accuracy and initial conditions, and it demands significant design and implementation effort—an approach we will not pursue here but instead reserve as a potential direction for future work should anyone be interested.

Instead, we adopt a simpler strategy: an impulse-like, open-loop energy injection. This method involves rapidly spinning the reaction wheel and then braking or reversing it to “kick” the *Triangle* upright. It is computationally light, straightforward to implement, and well-suited for our system.

The impulse-like, single-shot swing-up strategy consists of three main stages, each with tunable parameters. First, the reaction wheel is spun up by applying a constant angular velocity for a fixed duration, allowing it to accumulate angular momentum. This spin-up phase can involve either a gradual acceleration or direct velocity set-point control. To mitigate overshoot, the target angular velocity can be made a function of the initial rest angle of the *Triangle*. Next, a sudden deceleration of the wheel transfers the accumulated momentum to the body. This is typically achieved via braking or reversing the wheel’s direction. The aggressiveness of this deceleration—whether abrupt or gradual—affects the strength and smoothness of the resulting lift. Finally, if the momentum transfer is effective, the body swings upward toward the upright position, where the stabilizer can be activated to take control.

### 3.4.1 Determination of the wheel’s speed for swing-up

In this section, we determine the minimum initial angular rate that the reaction wheel must achieve before braking to safely approach the unstable equilibrium. The optimal angular rate for the reaction wheel during swing-up must balance energy injection, system dynamics, and overshoot avoidance. We utilize two fundamental physical principles governing the *Triangle*: conservation of energy and momentum exchange. Throughout this analysis, we neglect motor friction and assume instantaneous deceleration<sup>2</sup>.

#### Conservation of Energy

The kinetic energy of the rotating reaction wheel drives the change in potential energy of the *Triangle* body during swing-up.

Assume the *Triangle* starts at rest with initial angle  $\theta_0$ . To pump energy into the system via the reaction wheel’s kinetic energy such that the angle approaches zero, the required potential energy change is:

$$\Delta U = Mg(-\cos \theta_0 + \cos 0) \leq \frac{1}{2} I_w \dot{\phi}^2$$

Let  $\dot{\phi}_0$  be the minimum initial angular velocity of the reaction wheel needed to achieve this energy transfer after braking:

$$\begin{aligned} \Delta U &= \frac{1}{2} I_w \dot{\phi}_0^2 = Mg(1 - \cos \theta_0) \\ \implies \dot{\phi}_0 &= \sqrt{\frac{2MgL(1 - \cos \theta_0)}{I_w}} \end{aligned}$$

This expression provides a baseline lower bound for the initial angular velocity of the reaction wheel. However, it doesn’t account for the dynamics of how energy transfers from the wheel to the *Triangle* body, particularly during momentum exchange.

---

<sup>2</sup>I am very eager to generalize this analysis for non-zero motor friction and finite deceleration time after first validating these simplified results in simulation with Himanshu. -rms

## Momentum Transfer Dynamics

The angular momentum conservation for the *Triangle* system is:

$$(I_b + I_w)\dot{\theta} + I_w\dot{\varphi} = 0$$

When the wheel brakes suddenly, its momentum transfers to the body, producing an angular velocity:

$$\dot{\theta} = -\frac{I_w}{I_b + I_w}\dot{\varphi}$$

As the body's kinetic energy converts to potential energy during the rise, the peak angle  $\theta_p$  satisfies:

$$\begin{aligned} \frac{1}{2}(I_b + I_w)\dot{\theta}^2 &= Mg(1 - \cos \theta_p) \\ \frac{I_w^2\dot{\varphi}^2}{2(I_b + I_w)} &= Mg(1 - \cos \theta_p) \\ \theta_p &= \cos^{-1} \left( 1 - \frac{I_w^2\dot{\varphi}^2}{2(I_b + I_w)Mg} \right) \end{aligned}$$

For small angles ( $\theta_p \approx 0^\circ$ ), using the Taylor series approximation  $1 - \cos \theta \approx \theta^2/2$ :

$$\theta_p \approx \sqrt{\frac{I_w^2\dot{\varphi}_0^2}{(I_b + I_w)Mg}}$$

This analysis captures the transient swing-up behavior and predicts the body's state after wheel braking, which depends on the system parameters (masses and inertias).

## Implementation Procedure

The energy conservation approach gives us a fundamental lower bound on the required wheel speed for swing-up, but it's inherently a static analysis—it tells us whether there's enough energy in the system, but not how that energy actually moves or is transferred. On the other hand, using momentum transfer through the system's differential equations of motion makes the dynamic interaction between the wheel and the body much more explicit. This setup naturally includes motor dynamics as well: the motor torque  $\tau_m(t)$  shows up directly in the angular momentum equations, the electrical behavior is described by  $Li + Ri = V - k_e\dot{\varphi}$ , and the link between torque and current is given by  $\tau_m = k_t i$ . Time-varying inputs like braking profiles can also be handled through  $\dot{\varphi}(t)$ . So while energy analysis gives us a simple scalar condition, the momentum-based approach adds temporal resolution, which is key for modeling motor behavior, accounting for power electronics limits, and designing realistic braking strategies—all of which are important for real-world simulation and implementation.

Having performed the analysis following are the proposed implementation procedure, practicability of which is yet to be verified.

1. Calculate  $\dot{\varphi}_0$  from energy conservation
2. Verify if momentum transfer produces sufficient  $\theta_p$  for this  $\dot{\varphi}$
3. If necessary, increase  $\dot{\varphi}$  until both conditions are satisfied
4. Validate the process and the parameter through experimental testing

### 3.4.2 Determination of switching thresholds

Using a time-based threshold to switch from swing-up to stabilization is unsuitable because the system's motion depends on the *Triangle*'s initial orientation. The switching must occur late enough that the body approaches

upright with sufficient momentum but, at the same time, early enough for the stabilizer to act before the body falls away.

That being said, we have three possible parameters to use as thresholds for switching from swing-up to stabilization:  $\theta$  (body angle),  $\dot{\theta}$  (body angular velocity), and  $\dot{\varphi}$  (wheel speed). Among these,  $\theta$  and  $\dot{\theta}$  directly characterize the body's orientation and motion, making them the primary indicators for whether the system is near the upright position and slow enough for the stabilizer to engage effectively. The wheel speed  $\dot{\varphi}$ , while available, is optional—after all, during the momentum exchange process used in swing-up, the wheel is typically decelerated or even brought close to rest. By the time the body is upright, the energy transfer is largely complete, and the wheel's velocity provides little additional information about the body's readiness for stabilization. Therefore, relying on  $\theta$  and  $\dot{\theta}$  is both sufficient and more directly relevant to the switching decision. We are left with an important question:

*What should be the values of the thresholds for angle  $\theta_{th}$  and angular velocity  $\dot{\theta}_{th}$ ?*

We attempt to analytically estimate the switching thresholds  $\theta_{th}$  and  $\dot{\theta}_{th}$  by examining the region of attraction of the stabilizing controller around the upright position. The key idea is to ensure that, once the swing-up phase ends, the system's state lies within a neighborhood where the stabilizer can drive the state to equilibrium reliably.

Assuming a linear stabilizer, the linearized dynamics around  $\theta = 0$  can be used to compute the region in which the controller guarantees convergence. The linearized system is obtained by expanding the nonlinear equations around  $\theta = 0$  and  $\dot{\theta} = 0$ :

$$\ddot{\theta} \approx \frac{Mg\theta - \tau_m + \tau_f}{I}$$

This yields a linear approximation:

$$\ddot{\theta} = \frac{Mg}{I}\theta + \text{control terms}$$

The region of attraction of such a linear system can be bounded using a Lyapunov function or by simulating trajectories from various initial conditions and checking for convergence. In practice, a reasonable conservative estimate is to select  $\theta_{th}$  such that  $|\theta| < \theta_{max}$  and  $|\dot{\theta}| < \dot{\theta}_{max}$ , where  $\theta_{max}$  and  $\dot{\theta}_{max}$  are chosen so that the linear controller performs well within this domain.

These values will be determined by analyzing the eigenvalues of the linearized system matrix to determine bounds for stability and validated using simulations (i.e. sweep through  $(\theta, \dot{\theta})$  values and check convergence). This approach provides a more design-based method for selecting switching thresholds rather than relying purely on trial and error.

## 4 Learning Based Control (Experiments)

In this section, we seek to implement a neural network based controller for swing up and stabilization of the reaction wheel pendulum. Since, the wheel angle doesn't really play a significant role in evolving dynamics of the reaction wheel pendulum, only the three states of pendulum angle, pendulum velocity and wheel velocity is taken as input to the network which outputs a control value.

### 4.1 Data Generation from NMPC

The goal of our learning based Controller is to swing up and stabilize the system. However, the data that we seek to train our network is based on trajectories for finite time which is obtained as a minimization of the cost function. So, for this instance, a few techniques were implemented to see if we could make a pure behavior cloning neural network swing up and stabilize it(somewhat of workaround methods).

In NMPC, the controller solves a nonlinear program at each sampling step. The optimal control sequence is computed over the prediction horizon, but only the first control input is applied to the system, following the receding-horizon principle. The entire procedure is repeated at the next sampling instant with the newly measured state.

Consider the nonlinear dynamical system

$$\dot{x}(t) = f(x(t), u(t)), \quad (35)$$

with state vector

$$x = \begin{bmatrix} \theta \\ \dot{\theta} \\ \phi \\ \dot{\phi} \end{bmatrix},$$

and control input

$$u = \tau \quad (\text{torque}).$$

The state and control are subject to constraints

$$x_{\min} \leq x(t) \leq x_{\max}, \quad (36)$$

$$u_{\min} \leq u(t) \leq u_{\max}, \quad (37)$$

where  $x_{\min}, x_{\max}$  and  $u_{\min}, u_{\max}$  denote the admissible bounds on the state and control, respectively.

After discretization using a sampling period  $T_s$ , the system evolves according to

$$x_{k+1} = F(x_k, u_k), \quad k = 0, 1, \dots, N-1, \quad (38)$$

with the discrete-time constraints

$$x_{\min} \leq x_k \leq x_{\max}, \quad (39)$$

$$u_{\min} \leq u_k \leq u_{\max}, \quad (40)$$

where  $F(\cdot)$  denotes the discretized nonlinear dynamics.

### NMPC Optimization Problem

At each sampling instant, given the current state  $x_0 = x_{\text{meas}}$ , the NMPC solves the constrained finite-horizon problem

$$\min_{\{u_k\}_{k=0}^{N-1}} J = m(x_N) + \sum_{k=0}^{N-1} \ell(x_k, u_k), \quad (41)$$

$$\text{s.t. } x_{k+1} = F(x_k, u_k), \quad k = 0, \dots, N-1, \quad (42)$$

$$u_{\min} \leq u_k \leq u_{\max}, \quad k = 0, \dots, N-1. \quad (43)$$

Only the first optimal control action  $u_0^*$  is applied to the system, and the optimization is repeated at the next sampling step, following the receding-horizon principle.

### Objective Function

For our problem setup of Non-linear MPC, from our dynamics from Eqn. (2.3) , We set the friction torque equal to 0 and consider  $\tau_m$  to be equal to  $u$  as the control input. Also, the wheel angle term is not included in the cost function as it's not to be minimized nor to be used as a reference for control.

For our system,

Define the terminal (Mayer) cost

$$m(x_N) = Q_1 \theta_N^2 + Q_2 \dot{\theta}_N^2 + Q_3 (\dot{\phi}_N - \omega_s)^2, \quad (44)$$

and the stage (Lagrange) cost

$$\ell(x_k, u_k) = Q_1 \theta_k^2 + Q_2 \dot{\theta}_k^2 + Q_3 (\dot{\phi}_k - \omega_s)^2 + R u_k^2, \quad (45)$$

with weighting parameters chosen as

$$Q_1 = 1000, \quad Q_2 = 5, \quad Q_3 = 1, \quad R = 1.$$

Closed Loop trajectories obtained from the solution of this NMPC problem , were used as dataset for training the neural network.

In this Setup, we are attempting to train a neural network that infinitely stabilizes a system based on a dataset and for our specific problem , the control input slowly diminishes to zero while the pendulum attempts to reach the upright position , to counteract this in an attempt to let the pendulum overshoot the upright position and and let it balance there , by considering the specific dynamics of our system from Eqn.(12) , I introduce a time varying tracking reference to the wheel in the objective function so that it would force somewhat of a bang bang behavior around upright.

For that , we design the wheel velocity reference such that

$$w_{\text{ref}} = A \cdot \sin(bt + \alpha)$$

We want this to fluctuate between -A to +A in each time step in NMPC trajectory generation which creates the oscillatory behavior, For that we simply solve the linear equations of

$$\begin{aligned} b \cdot t_{\text{step}} + \alpha &= \frac{\pi}{2} \\ b \cdot 2t_{\text{step}} + \alpha &= \frac{3\pi}{2} \end{aligned}$$

Further, we wish to choose the value of A such that it only results in say x% of maximum possible control. To determine the magnitude A , using Eqn.(12) and substituting to be x% of maximum control limit and letting equal to 0 around the upright

$$I_w \frac{2A}{t_{\text{step}}} = u$$

However, performing the experiments with this , the swingup and stabilization is performed neatly but the wheel velocity slowly drifts higher and higher leading to actuator saturation. Instead of this exact design , when I did try it with wheel velocity fluctuating around some value  $w_s$  it did show the behavior of balancing with the wheel velocity settling to a fixed value but it suffered from the problem of distributional shift and only worked with either just positive angles only or negative angles only. This wasn't pursued any further.

## 4.2 Imitation Learning Approaches

### Behavior Cloning Controller

A behavior cloning controller just learns a mapping from states to expert actions by treating control as a supervised learning problem.

For our system, the network maps the current state of the system to a control action by passing the input through two hidden layers of 64 neurons each, using ReLU activations, and outputs a single control value which is based on supervised loss.

### DAGGER Algorithm

DAGGER (Dataset Aggregation) [3] tackles the core flaw of basic behavioral cloning: the policy only sees expert states, so it falls apart when its own mistakes push it into unseen regions. DAGGER fixes this by repeatedly rolling out the learned policy, collecting the states it actually visits, and asking the expert to label those states with the correct actions. Each iteration augments the training set with these new expert-labeled samples, gradually covering the full distribution induced by the learned policy rather than the narrow distribution of expert demonstrations.

## **Q-loss**

This is an approach to imitate NMPC as introduced in the paper [2] in which instead of supervised learning from control inputs , the NMPC problem is solved for each state/ input to the network while training while introducing a constraint that fixes the first control to the network predicted control and the cost function value is used as the loss and the lagrange multiplier corresponding to the constraint that fixes first control to the network predicted control which happens to be equal to gradient of the cost function with respect to this network predicted first control input is used as the gradient for backpropagation in the neural network.

## **References**

- [1] Elektor International Media. Elektor Magazine, may/june 2016, no. 332. *Elektor Magazine*, May 2016. Digital issue, Elektormagazine.com.
- [2] Andrea Ghezzi, Jasper Hoffman, Jonathan Frey, Joschka Boedecker, and Moritz Diehl. Imitation learning from nonlinear mpc via the exact q-loss and its gauss-newton approximation. In *2023 62nd IEEE Conference on Decision and Control (CDC)*, pages 4766–4771, 2023.
- [3] Stephane Ross, Geoffrey Gordon, and Drew Bagnell. A reduction of imitation learning and structured prediction to no-regret online learning. In Geoffrey Gordon, David Dunson, and Miroslav Dudík, editors, *Proceedings of the Fourteenth International Conference on Artificial Intelligence and Statistics*, volume 15 of *Proceedings of Machine Learning Research*, pages 627–635, Fort Lauderdale, FL, USA, 11–13 Apr 2011. PMLR.